AD 420941

UNCLASSIFIED

SSD-TDR-63-193

Experimental Results on the Combustion Rate of Graphite Exposed to a Plasma-Arc Flow

31 AUGUST 1963

Prepared by W. E. WELSH, JR.
Aerodynamics and Propulsion Research Laboratory

Prepared for COMMANDER SPACE SYSTEMS DIVISION
UNITED STATES AIR FORCE
Inglewood, California

LABORATORIES DIVISION

CONTRACT NO. AF 04(695)-269

SSD-TDR-63-193

Report No.
TDR-269(4230-40)-1

EXPERIMENTAL RESULTS ON THE COMBUSTION RATE OF GRAPHITE EXPOSED TO A PLASMA-ARC FLOW

Prepared by

W. E. Welsh, Jr.
Aerodynamics and Propulsion Research Laboratory

AEROSPACE CORPORATION
El Segundo, California

Contract No. AF 04(695)-269

31 August 1963

Prepared for

COMMANDER SPACE SYSTEMS DIVISION
UNITED STATES AIR FORCE
Inglewood, California

SSD-TDR-63-193

Report No.
TDR-269(4230-40)-1

EXPERIMENTAL RESULTS ON THE COMBUSTION RATE OF GRAPHITE EXPOSED TO A PLASMA-ARC FLOW

Prepared by:

W. E. Welsh, Jr.

W. E. Welsh, Jr.

This technical documentary report has been reviewed and is approved for publication and dissemination. The conclusions and findings contained herein do not necessarily represent an official Air Force position.

For Space Systems Division
Air Force Systems Command:

Gladstone S. Lewis, Jr.

For Laboratories Division
Aerospace Corporation:

Harold Mirels

H. Mirels, Head
Advanced Propulsion and Fluid Mechanics Department

J. G. Logan, Director
Aerodynamics and Propulsion Research Laboratory

AEROSPACE CORPORATION
El Segundo, California

ABSTRACT

Experimental data are presented on the combustion rate of ATJ-graphite specimens at surface temperatures from 1600 to 4100°R. The specimens were flat-faced cylinders in a subsonic stagnation-point air flow from a 200-kW electric plasma arc. A comparison is made with the recent theoretical results of Welsh and Chung for the combustion of graphite under conditions where the effects of boundary layer diffusion and heterogeneous kinetics are both significant in limiting the combustion rate. The comparison indicates qualitative agreement between theory and experiment. The combustion rate varied over an extended range, the lower portion of which is ascribed to the well-recognized effect of heterogeneous kinetics, and the upper portion is believed to reflect a change in the effective product of combustion at the surface.

CONTENTS

NOMENCLATURE ix

I. INTRODUCTION 1

II. EXPERIMENTAL APPARATUS 5

A. Type A Specimen 7

B. Type B Specimen 7

C. Type C Specimen 9

III. EXPERIMENTAL PROCEDURE 11

IV. EXPERIMENTAL RESULTS 13

A. Specimen Temperatures 13

B. Heat Flux 19

C. Specimen Length and Mass Loss 20

D. Influence of Cathode Particles 20

E. Combustion Rate as a Function of Surface Temperature 21

F. Comparison with the Data of Diaconis, Gorusch, and Sheridan 21

G. Comparison with the Data of Golovina 23

H. Comparison with Cold-Air Data 25

V. CONCLUDING REMARKS 27

APPENDICES

A. Theoretical Heat Flux and Combustion Rate Calculations 29

B. Estimation of Experimental Errors 31

REFERENCES 37

FIGURES

1	Theoretical Results	4
2	Experimental Configuration	6
3	Specimen Configurations	8
4	Views of Type C Specimen Test	10
5	Recorded Parameters for a Typical Test	12
6	Sample Starting Temperature	14
7	Steady-State Specimen Temperature Profile	16
8	Heat Flux Comparison	18
9	Experimental Combustion Rates	22
10	Comparison with Other Investigations	24

TABLE

1	Experimental Results	15

NOMENCLATURE

A_1, A_2	constants defined in Ref. 3
C	$(\rho_w \mu_w / \rho_e \mu_e)^{0.2}$
C_1	oxygen mass fraction
c_p	specific heat
d	diameter
h_D	dissociation energy
h_s	free-stream enthalpy
k	thermal conductivity
L	specimen length
Le	Lewis number
M	molecular weight
m	mass flux
n	reaction order, number of computation segments, or number of moles
P	external pressure
Pr	Prandtl number
q	heat flux
R	gas constant or Rankine temperature
Sc	Schmidt number
T	temperature
t	time
u	velocity normal to surface
x	axial distance in specimen

NOMENCLATURE (Continued)

α	thermal diffusivity
β	inviscid velocity gradient
ϵ	body shape parameter
μ	viscosity
ρ	density

Subscripts and Superscripts

$(\overline{\ \ })$	average
d. l.	diffusion-limited
e	external
i	general designation
j	jet
ref.	reference at CO d. l.
s	stagnation point
w	wall

I. INTRODUCTION

The entry of a space vehicle into a planetary atmosphere is accompanied by severe heating of the vehicle surface by the shock-heated gases surrounding the vehicle. This heating produces high surface temperatures which may involve melting, sublimation, or combustion of the surface material, depending on the nature of the material and the gaseous environment. Reinforced plastic materials considered for re-entry heat shields decompose upon rapid heating to a porous graphitic structure much like charcoal. Dense artificial graphites are also considered for re-entry heat shields; pyrolytic graphite is attractive because of its anisotropic thermal conductivity. The surface recession rate of a graphite material under re-entry conditions depends upon either the combustion rate of the material with the atmospheric gases, or the sublimation rate of the material. These rates, in turn, depend on the combined characteristics of the material and the gaseous environment. The surface recession rate is important because it affects the aerodynamic shape of the vehicle, the thickness of the heat shield, and the degree of thermal protection provided for the vehicle.

Graphite sublimation rates are generally negligible for surface temperatures below $6000^{\circ}R$, as noted by Scala (Ref. 1), for entry into the earth's atmosphere where the material may burn with oxygen. The surface temperature of an ablative heat shield on a ballistic vehicle entering from an earth orbit is generally in a range such that the surface burns at a rate corresponding to the maximum rate at which oxygen can diffuse to the surface. Lifting re-entry trajectories involve lower heat transfer rates and lower surface temperatures, however, and it has been shown (Ref. 1) that for this case the combustion rate may depend on the kinetics of the heterogeneous reaction at the surface between carbon and oxygen.

Welsh and Chung (Ref. 2) have recently performed a boundary-layer analysis of the combustion rate of graphite at the stagnation region of a re-entry vehicle for a range of conditions between the kinetic-limited and the diffusion-limited extremes. This analysis was performed using a closed-form approximation for existing solutions showing the effect on the mass-transfer rate of mass addition to a boundary layer. The results were shown for Schmidt numbers of 0.514 and 0.72 and bracketed, at the diffusion limit, the results of a more extensive boundary-layer diffusion analysis of combustion by Scala (Ref. 1). The results for Sc = 0.514 were 13 percent higher than Scala's result; the Sc = 0.72 result was 12 percent lower than Scala's. These comparisons were made for a stagnation-point surface at 2000 to 4000°R, with carbon-monoxide assumed to be the only product of the surface combustion. The transition from kinetic-limiting to diffusion-limiting conditions of combustion was described in terms of a Damkohler number that was a measure of the relative diffusion and reaction times.

In a later analysis, Welsh and Chung (Ref. 3) investigated a possible interaction between the kinetic-diffusion transition and the thermochemical equilibrium of gaseous species at the burning surface. Here a choice had to be made between the following equilibria at the surface:

$$CO_2(g) + C(s) \leftrightarrows 2\ CO(g) \tag{1}$$

$$2\ CO_2(g) + M \leftrightarrows 2\ CO(g) + O_2(g) + M \tag{2}$$

The catalyst M in equilibrium (2) represents the carbon surface. Scala (Ref. 1) has utilized equilibrium (1) in an analysis of graphite combustion under diffusion-limited conditions. It was shown in Ref. 3 that equilibrium (2) may be preferable in the kinetic regime, where equilibrium (1) becomes questionable because of kinetic limitations. The essential difference between the results of the two equilibria is in the effect of oxygen concentration on the $CO:CO_2$ concentration ratio at the surface. The $CO:CO_2$ ratio at the surface determines the level of the diffusion-limited combustion rate, within a factor of two. Scala's results (Ref. 1) for the intermediate (kinetic-diffusion) regime, calculated by an approximate series-resistance method, showed that CO was always the predominant species at the surface at the diffusion limit. The surface oxygen concentration at the diffusion limit was calculated secondarily by the application of equilibrium (2) after the $CO:CO_2$ ratio was determined from equilibrium (1).

The results of Welsh and Chung (Ref. 3) for the intermediate regime showed that, with equilibrium (2), the kinetic-diffusion transition usually involved predominantly CO_2 at the surface and that at some higher temperature the surface species changed to CO. These results are shown in Fig. 1 (reproduced from Ref. 3) for several re-entry flight conditions of a 1-ft nose-radius vehicle. Examples of three classes of transitions are shown in the figure. These are defined as: Class 1, a kinetic-diffusion transition with CO_2 effective product at the surface; Class 2, a product-transition from CO_2 to CO with increasing surface temperature in the diffusion-limited regime; Class 3, a merging of Class 1 and 2 transitions. Had equilibrium (1) been utilized in these calculations the relative combustion rate would go from zero to unity in the temperature range shown for the Class 1 transitions. Thus, for a given material and flow condition, equilibrium (2) causes the combustion rate to vary significantly over a much larger temperature range than does equilibrium (1).

It was felt that, to investigate the validity of the product-transition indicated by the analysis, a graphite-air combustion experiment should be performed in the range of conditions where surface kinetics and boundary layer diffusion are simultaneously important. The experiment was performed and is the subject of this report.

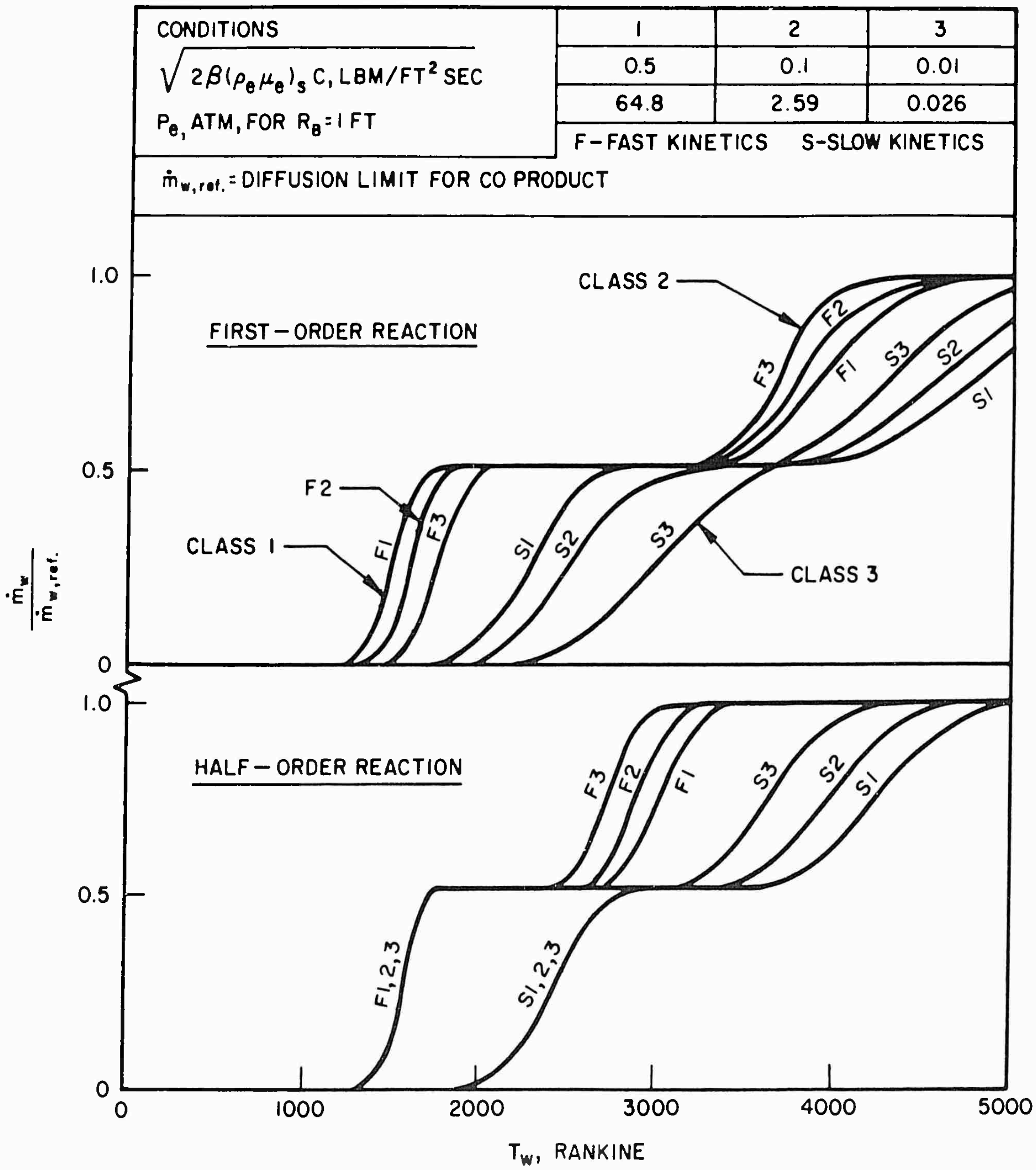

Fig. 1. Theoretical Results

II. EXPERIMENTAL APPARATUS

The stagnation-point flow region of a re-entry vehicle was simulated in these experiments by the normal impingement of a hot, circular, subsonic air jet on a graphite specimen surface. The air jet comprised the exit flow of a 200-kW (nominal maximum gross power) electric plasma arc. This arc is a two-chamber unit, in which the first chamber consists of primary air injection ports, a cylindrical graphite cathode on the axis, and a copper anode surrounding the cathode. The second chamber is a plenum in which the primary air is mixed and equilibrated with secondary air injected in the plenum, or simply equilibrated without secondary air injection before ejection to the ambient. The arc and its associated apparatus are described in detail in Ref. 4.

John and Bade (Ref. 5) have described the method of subsonic plasma-arc simulation of hypersonic stagnation-point flows and conclude that the available data indicate that this method offers attractive simplifications for heat-transfer experiments in this regime. Horn and Lafazan (Ref. 6) have reported ablation experiments performed in the Aerospace 200-kW arc facility using the subsonic jet technique.

The experimental flow configuration is shown schematically in Fig. 2. The plasma-arc nozzle exit diameter was 1/2 in., and the nozzle-to-specimen axial spacing was 1.5 in. All specimens were provided with a relatively large-diameter guard plate around the specimen to maintain the flat-plate-impingement configuration and to promote one-dimensional phenomena in the specimens. The specimens used in the experiments were machined from an ATJ-graphite block of density 1.76 g/cc. Three types of specimen configurations and mountings were used in order that the experiments could be performed over a significant range of surface temperatures. The surface temperature was controlled by varying the sample thickness and cooling the rear face. The specimen configurations are shown in Fig. 3.

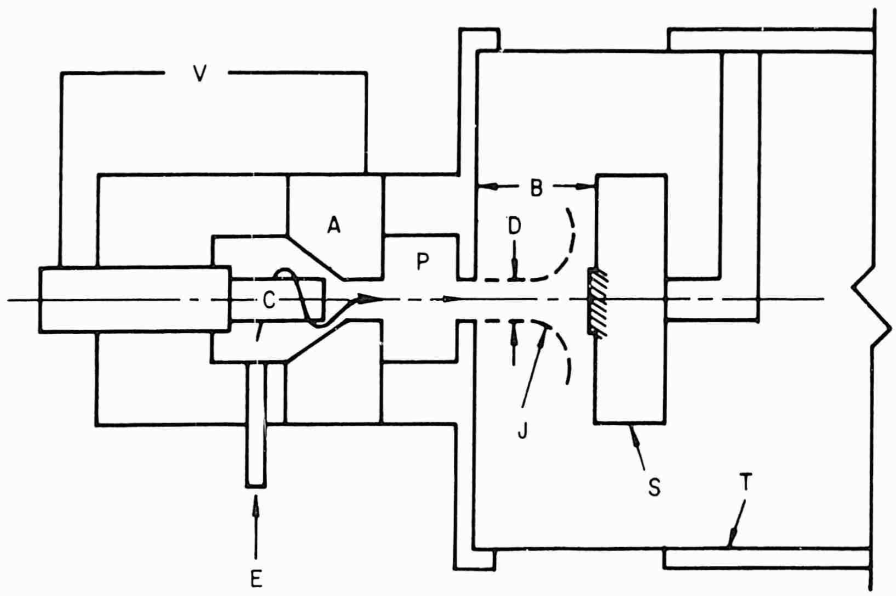

A ANODE
B 1.5 IN. SPACING
C CATHODE
D 0.5 IN. DIAMETER
E AIR INJECTION
J JET OUTLINE
S SPECIMEN ASS'Y
T TUNNEL WALL (TUNNEL OPEN TO AMBIENT)
V ARC VOLTAGE
P PLENUM

Fig. 2. Experimental Configuration

A. TYPE A SPECIMEN

Type A specimens were used in tests at surface temperatures between 1500 and 2700°R. The specimen was 0.45 in. long and 0.75 in. in diam, with an integral 0.10-in. flange at the base. A thermocouple was installed in the base flange. The specimen was clamped between a copper calorimeter and the inner lip of the copper guard plate, with a lava ring installed to minimize heat loss to the guard plate. The heated face of the specimen protruded 0.050 in. from the front surface of the guard plate to allow for recession of the specimen during combustion, without a significant change in the flow condition. Porcelain cement was cast in the 0.020-in. radial space between the specimen and the guard-plate inner lip to prevent gas flow around the specimen. In several tests, thin sheets of stainless steel were inserted between the specimen and the calorimeter face to increase the specimen temperature. The water flow rate and temperature rise through the central calorimeter were monitored for each test. The guard plate was water-cooled, but the heat load was not monitored.

B. TYPE B SPECIMEN

Type B specimens were used in tests at surface temperatures between 2300 and 3000°R. The rear face of the specimen was an integral part of the calorimeter coolant passage and was clamped to the calorimeter by means of a threaded flange. Diffusion of water coolant into the graphite specimen was prevented by installing a thin aluminum-foil disk at the rear face. The length of the specimens ranged from 0.50 to 1.3 in., depending on the desired surface temperature; the diameter of the main body was 0.75 in. One or more thermocouples were installed radially at various positions along the length of the specimen. The 0.020-in. radial space between the specimen diameter and the inner surface of the guard-plate inner lip was filled with porcelain cement. Calorimetry was the same as on Type A specimens.

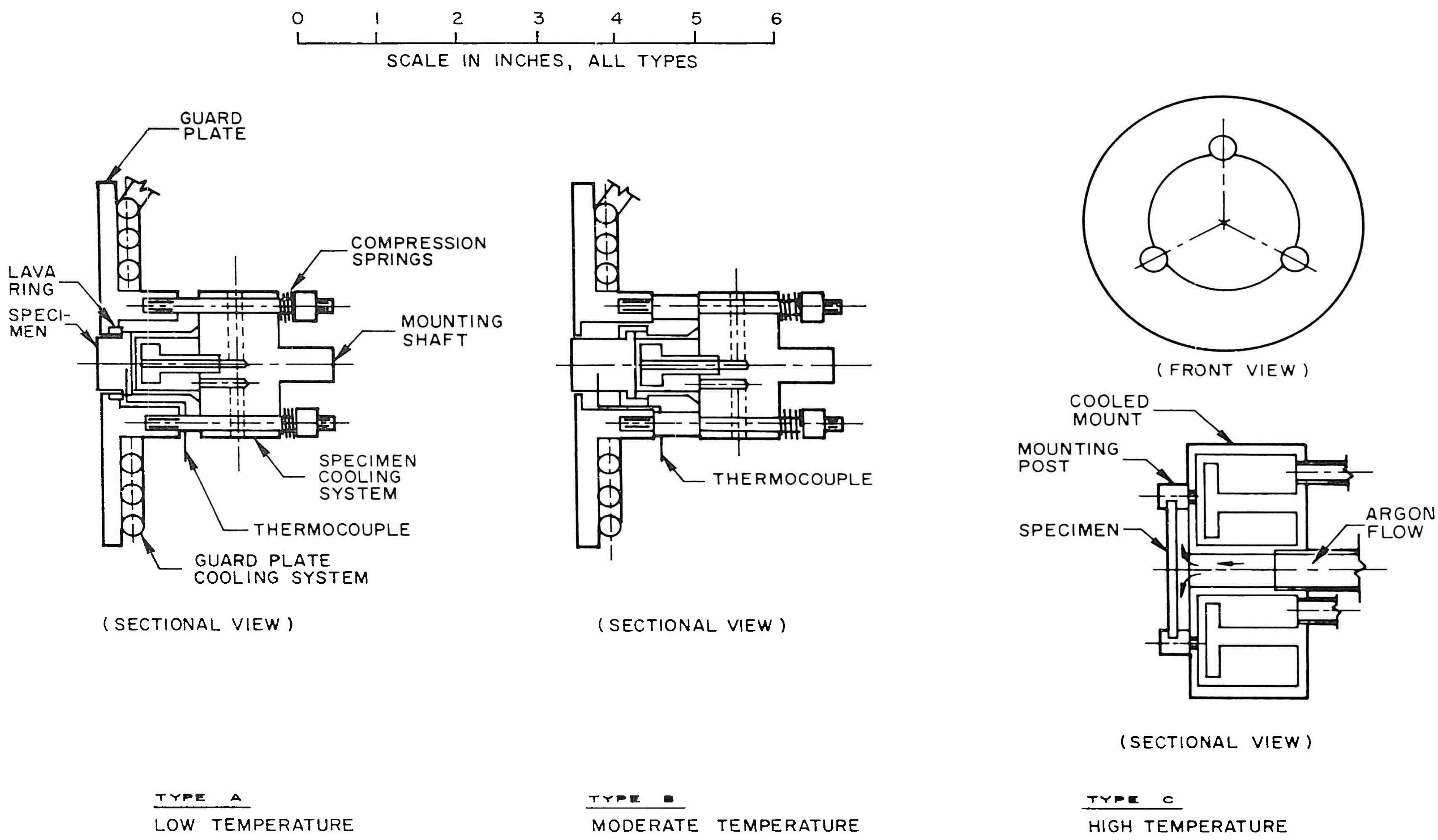

Fig. 3. Specimen Configurations

C. TYPE C SPECIMEN

Type C specimens were used in tests at surface temperatures near 4100°R, which was the radiation equilibrium temperature for the convective conditions of these tests for a sample radiating heat from both sides. The specimen diameter was 1.5 in.; the thickness was 0.125 in. The specimen disk was held by three slotted posts at 120 degree intervals, at an axial distance of 0.125 in. from a water-cooled copper guard plate. A central jet of argon was directed against the rear surface of the specimen to prevent oxidation of that face. Several tests were conducted to check the effect of sample stand-off distance, mounting-post configuration, and argon flow rate on the temperature and front-face combustion rate of the specimen. These tests indicated that the configuration selected had no undesirable effect on the primary variables of the experiments. The surface temperature (front face) was determined by manual measurement with a monochromatic optical pyrometer utilizing a beam reflected by a mirror installed on the rear face of the arc housing.

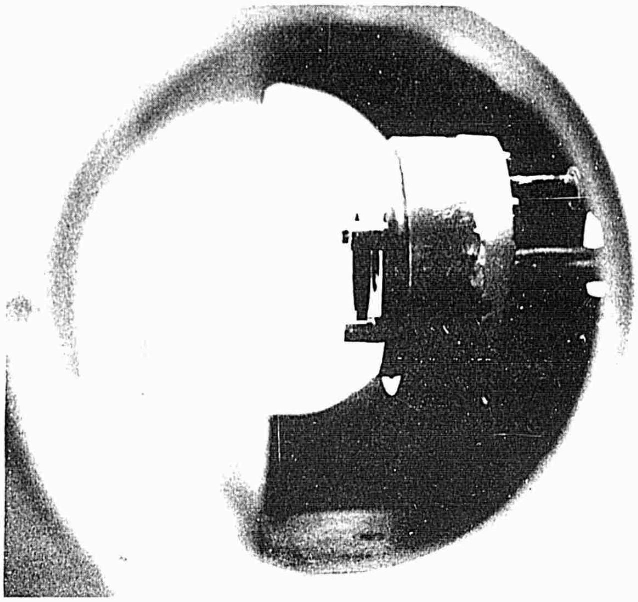

a) Before Test

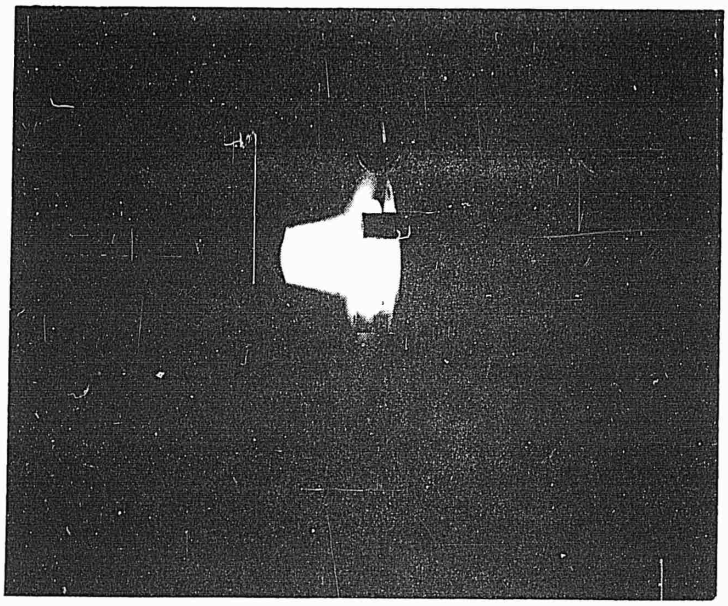

b) During Test

Fig. 4. Views of Type C Specimen Test

III. EXPERIMENTAL PROCEDURE

The procedure for conducting a typical experiment was as follows:

1) The specimen and its holder were positioned downstream of the plasma arc.

2) The cooling water to the specimen and guard plate cooling passages were turned on.

3) The cooling water temperature-rise thermocouples and the specimen interior thermocouple were connected to recording potentiometers.

4) The plasma arc was operated for 60 sec at a nominal condition of 2 g/sec air flow and outlet enthalpy of 4060 Btu/lbm.

5) The specimen was removed, weighed, and measured for dimensional changes.

6) The records of arc operating conditions and specimen operating conditions, i. e. , coolant flow rate, temperature rise, and internal temperature, were analyzed to determine the average (one-dimensional) heat flux through the specimen, the average specimen surface temperature during the test, and the theoretical heat flux for the average arc operating condition.

Photographs taken just prior to and during a combustion experiment with a Type C specimen are presented in Fig. 4.

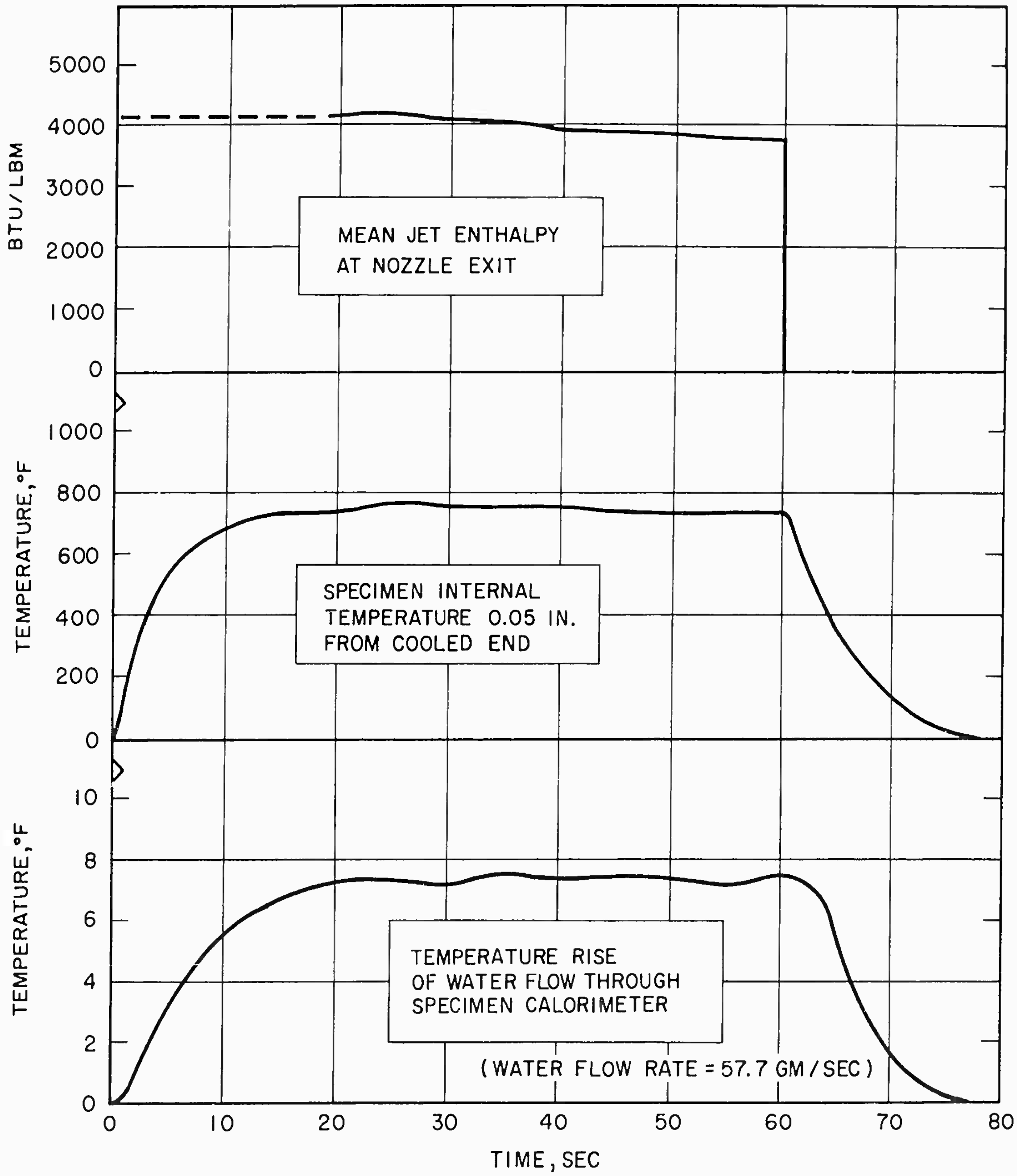

MEAN VALUE OF OTHER PARAMETERS:

ARC VOLTAGE — 82 V
ARC CURRENT — 950 amp
ARC GROSS POWER — 80 kW
ARC NET POWER — 19 kW
AIR FLOW RATE — 2.1 GM / SEC
PLENUM PRESSURE — 1.05 IN. HG. GA.

(DATA OF TEST NO. 9 – TYPE A SPECIMEN)

Fig. 5. Recorded Parameters for a Typical Test

IV. EXPERIMENTAL RESULTS

The experimental results for those tests that were considered of acceptable quality are given in Table 1. Several tests were invalidated because of equipment breakdowns or because of the developmental nature of certain early versions of the specimen configuration and are not reported in Table 1.

A. SPECIMEN TEMPERATURES

Typical recordings of significant operating parameters during a test (of Types A and B specimens) are shown in Fig. 5. It may be noted that the recorded specimen temperature and heat load demonstrated a slow approach to the steady-state condition in the initial 20 sec of the test. It was determined that the energy increment of this lag corresponded closely to the difference between the enthalpies of the graphite sample at steady state and at room temperature. The calorimeter body (through which the sample transferred heat) absorbed negligible heat in the starting period. The approximate temperature profiles considered to exist in a Type A sample during a test are shown in Fig. 6. These transient temperatures were calculated for the particular test conditions of heat flux and average sample properties, using the solution of Carslaw and Jaeger (Ref. 8) for a plate cooled on one face and heated at constant flux on the opposite face. These profiles are somewhat idealized in that they do not indicate the small amount of radial heat loss from the specimen to the guard-plate inner lip, the effect of local temperature on conductivity, or the rise of the rear-face temperature required to transfer heat to the calorimeter. Since the objective in a typical experiment was to determine the combustion (graphite mass loss) rate at a particular value of surface temperature, the variation of surface temperature during the starting period was undesirable, but could not be avoided. The profiles in Fig. 6 were calculated using conservative values of conductivity and diffusivity (as specified in the figure)

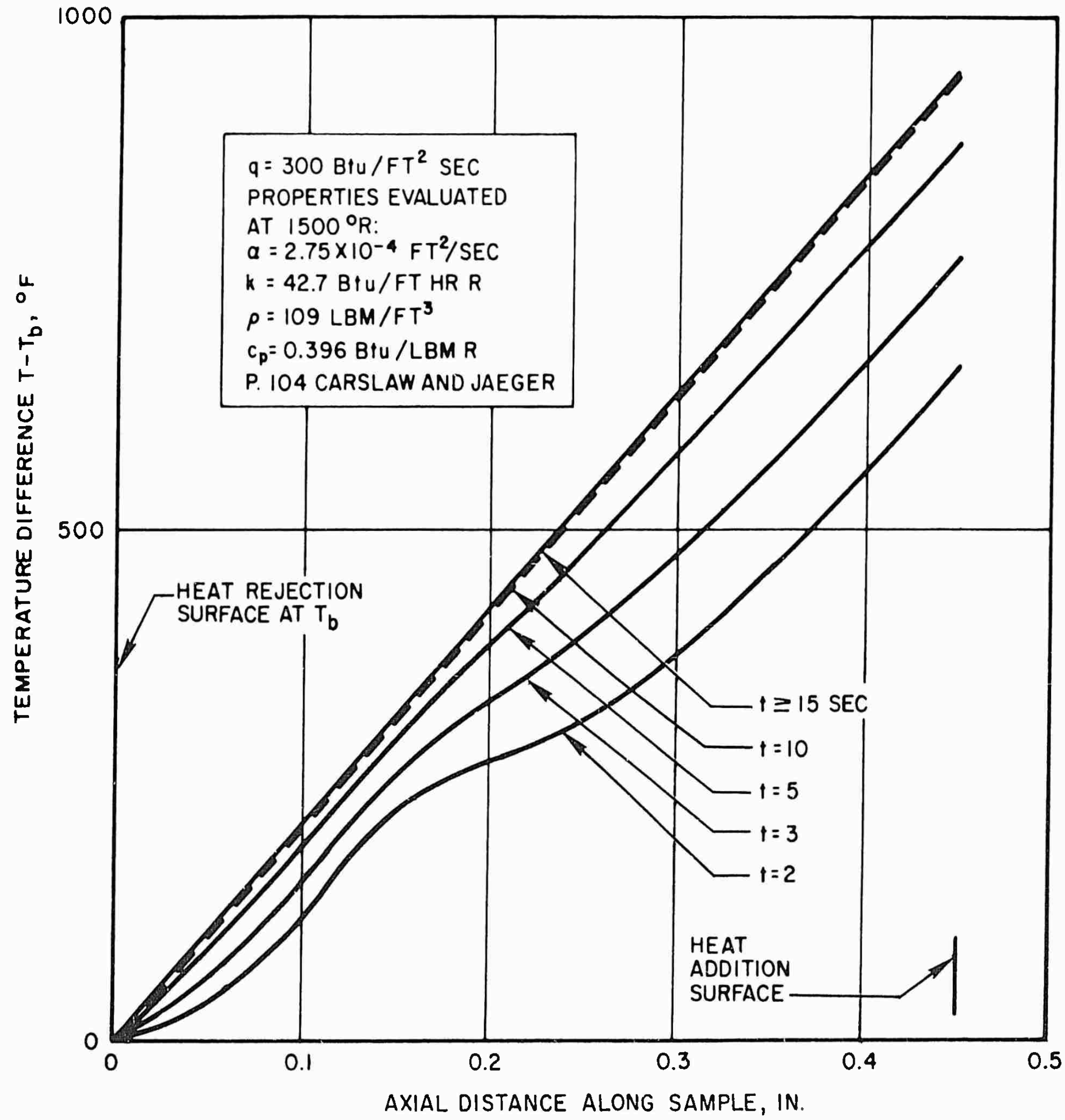

Fig. 6. Sample Starting Temperature

Table 1. Experimental Results

Test Number	Initial Specimen Length, in.	Specimen Mass[a] Loss Rate $\dot{m}_w$, $lbm/ft^2\ sec \times 10^3$	Surface Temperature, ^oR	Air Flow Rate, g/sec	Air Enthalpy,[b] h/RT_o	Experimental Heat Flux,[c] $Btu/ft^2\ sec$	Specimen Type
1	0.450	5.96	2050	2.13	102	331	A
2	0.450	7.86	2600	2.03	114	238	A
3	0.450	8.64	2700	2.08	127	208	A
4	0.450	4.31	1960	2.08	123	301	A
5	0.449	4.85	1910	2.04	104	302	A
6	0.450	2.33	1680	1.91	125	287	A
7	0.449	3.02	1620	2.10	125	310	A
8	0.437	2.72	1610	2.10	108	300	A
9	0.451	6.06	2080	2.10	112	306	A
10	1.017	5.37	2310	1.99	126	230	B
11	1.257	8.42	2645	2.08	130	193	B
12	0.845	6.32	2520	1.85	120	289	B
13	1.180	9.57	2926	1.78	120	210	B
14	0.125	12.4	4050	2.02	120		C
15	0.125	10.33	4060	1.92	116		C
16	0.125	10.78	4100	1.92	119		C
17	0.125	10.80	4150	1.93	120		C

[a] Wall mass loss rate calculated from length loss and corrected for cathode particle impingement by $+ 1.2 \times 10^{-3}$ $lbm/ft^2 sec$.

[b] $RT_o = 33.86$ Btu/lbm.

[c] To specimen calorimeter only; no measurement on Type C specimen.

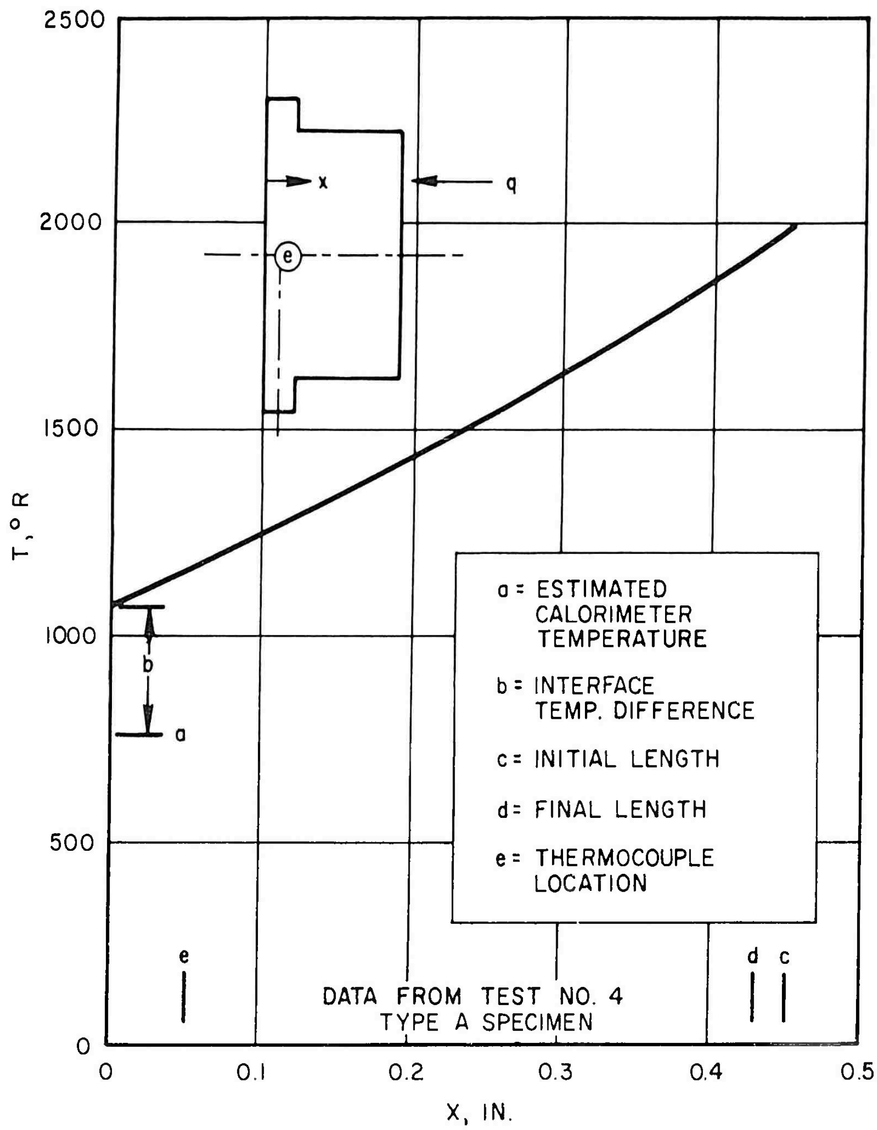

Fig. 7. Steady-State Specimen Temperature Profile

and therefore the lag time of surface temperature shown is a conservative estimate. Since the standard sample test period was 60 sec, the dimensionless lag time (using 2/3 of the surface temperature rise as an indicator) was 3/60, which is reasonable in comparison with the anticipated over-all experimental accuracy.

Figure 7 shows the approximate steady-state temperature distribution in a Type A specimen for a typical test. The nonlinearity is due to the temperature-dependent thermal conductivity of graphite. A stepwise numerical procedure was used for this calculation, based on the measured heat load through the sample, the measured temperature near the rear face, and one-dimensional conduction through the specimen. Again the heat loss near the front surface to the guard-plate lip is neglected, since this loss was believed to exert a negligible influence at the surface temperatures prevailing with the Type A specimens. The justification for this is based on the measurement of heat flux; the Type A configuration tests indicated heat flux values identical (within five percent) to values measured using a relatively cold copper specimen substituted for the graphite specimen.

The surface temperatures of Type B specimens were also determined using the numerical conduction procedure, modified to account for radiative loss from the side of the specimen and a conduction heat loss to the guard-plate lip. The calculation procedure was checked against direct (thermocouple) temperature measurements in the sample near the surface and corrected when necessary. The surface temperature could not be measured directly, for several reasons. A thermocouple imbedded directly beneath the surface would have locally disturbed the temperature of the graphite, and would have become useless upon a slight recession of the burning surface. Pyrometric measurements were found to be subject to error at surface temperatures below $3000^{o}R$ because of radiation from the arc column approaching the specimen, and graphite particles released from the arc cathode.

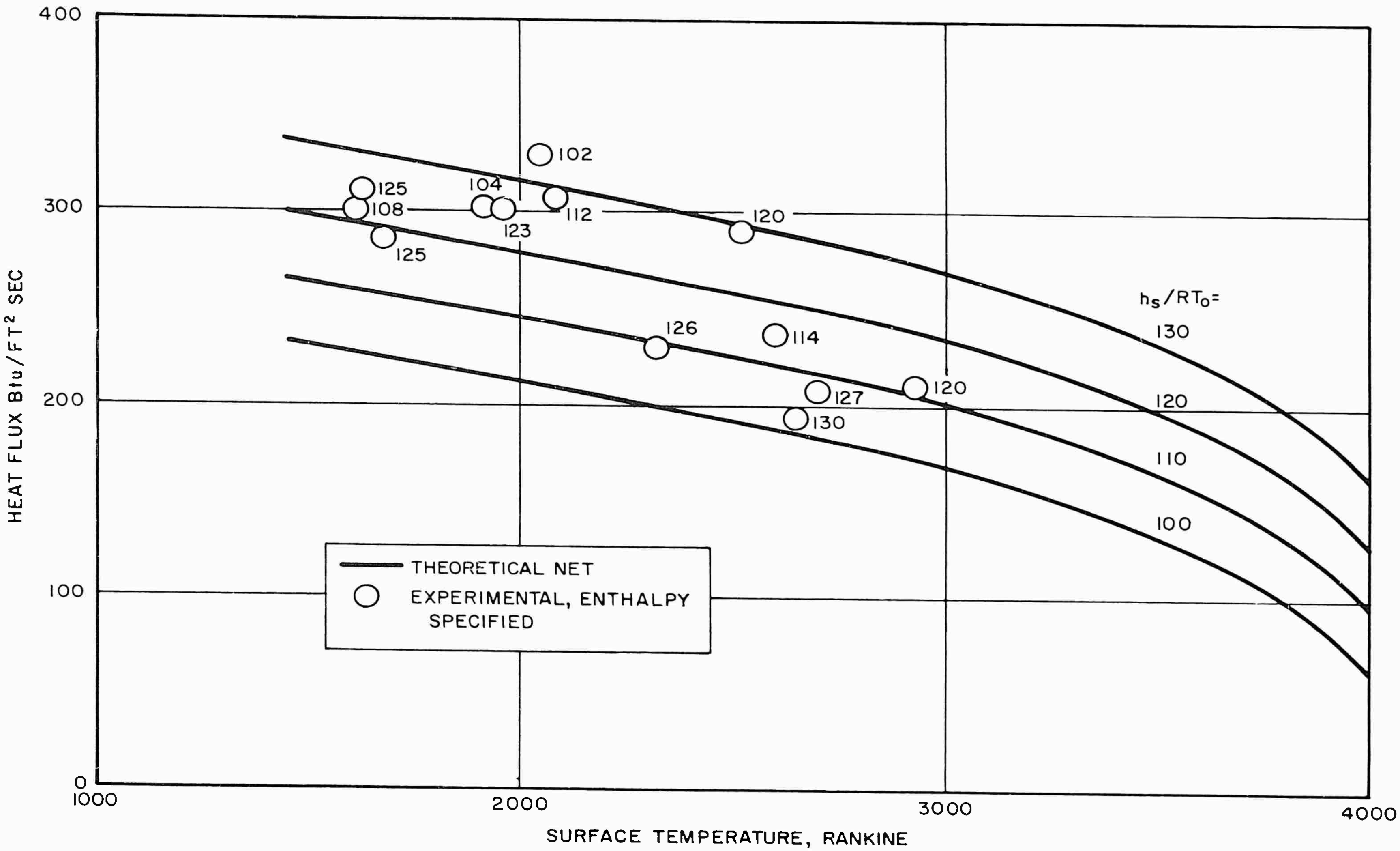

Fig. 8. Heat Flux Comparison

The surface temperatures of Type C specimens, measured pyrometrically, were found to correspond, within 50°R, to the radiation equilibrium temperature for these conditions.

B. HEAT FLUX

The primary reason for measuring the heat flux through the Type A and B specimens was to permit the calculation of the temperature of the heated surface. Secondarily, it is of interest to compare the measured heat flux with the theoretical value calculated for the jet conditions (see Appendix A). The experimental heat flux values are compared in Fig. 8, with theoretical curves for representative stagnation enthalpies. The theoretical heat flux values are shown for a noncombusting surface with an emissivity of 0.9. Modifications to these theoretical values, which would result from accounting for the effects of mass addition and carbon combustion heat generation, are not shown. These modifications are estimated to comprise a small positive correction between zero and 20 Btu/ft^{2}sec, depending on the rate of combustion. The experimental and theoretical heat flux values are in reasonable agreement at the lower surface temperatures (1600-2000°R), but a discrepancy of approximately 20 percent appears at higher temperatures. This decrease of experimental values at higher surface temperatures is believed to be the result of inadequate insulation between the specimen and the guard-plate lip, and requires that corrections be made to the calculated temperature, based on additional internal temperature measurements. The agreement with theory at lower temperatures indicates the actual non-dimensional jet enthalpy for all experiments was 125±5, whereas the values obtained from the arc heat balance were as low as 102. The value deduced from the measured heat flux is felt to be more accurate, and the lower heat-balance enthalpies are believed to have resulted from spurious changes in the arc instrumentation.

C. SPECIMEN LENGTH AND MASS LOSS

The fractional changes of length and mass for all specimens were found to be in good correspondence, generally within 10 percent, indicating the combustion of the graphite was confined to the exposed front surface, or a very thin layer at the surface. In most tests the front surface recessed one-dimensionally, with negligible assymmetry, and remained flat except for a slight rounding of the edges of the face. A slight central dishing of the Type C specimens occurred due to the failure of the stagnation-point similarity at larger radial distances, but a reasonably flat central region existed that permitted accurate analysis. Length loss of specimens was 0.050-in. or less in all tests; therefore, an initial 0.050-in. protrusion ensured that the specimen did not recede behind the front plane of the guard plate.

D. INFLUENCE OF CATHODE PARTICLES

The use of a graphite cathode in the plasma arc introduced two potentially serious errors into the experimental combustion results. First, the oxygen in the air flow may have been depleted; the maximum depletion is estimated at 19 percent, based on a nominal 3 percent contamination level. This calculation was based on the assumption that the entire carbon cathode loss went into molecular combination with oxygen as carbon monoxide. It is known that a large fraction of the cathode loss is in the form of large particles, probably 10 to 1000 microns in diameter, which do not burn completely before leaving the plasma arc. Thus the 19 percent calculated oxygen depletion is in excess of the actual depletion, perhaps by a factor of 3 or 4. Second, a fraction of these particles leaving the plasma arc have been observed to impinge on a combustion sample placed downstream of the arc exit, stick for some time, and radiate before cooling to the sample temperature. The particles then either remain stuck and burn, or are swept off. In preliminary experiments, graphite combustion samples at relatively low surface temperatures (determined by interior temperature measurements in a sample) were observed to gain both mass and length. In addition, the surface temperature observed pyrometrically under these conditions was erroneously high. The highest observed rate at which mass was added to the sample was 1.2×10^{-3} lbm/ft^{2}sec, which corresponded to about 3 percent of the cathode loss rate. The observed specimen combustion rates in the main series of experiments were in the range from 1×10^{-3} to 1×10^{-2} lbm/ft^{2}sec. It was felt that a more-or-less arbitrary correction should be made to the observed combustion rates, in which the corrected rate was the observed rate plus the particle addition rate. This correction was performed for all tests, with the correction term simply taken as the highest observed addition rate, 1.2×10^{-3} lbm/ft^{2}sec. No correction was made for oxygen depletion since it would have been quite arbitrary. It will be shown that the results of an experiment using an essentially uncontaminated plasma arc flow correspond closely to these results, which lends some confidence to the particle-addition correction and the omission of an oxygen-depletion correction for the present experiments.

E. COMBUSTION RATE AS A FUNCTION OF SURFACE TEMPERATURE

Figure 9 shows the measured combustion rates as a function of specimen surface temperature. For comparison, the theoretical combustion rates based on Refs. 2 and 3 (and discussed in Appendix A) are included in the figure. The theoretical rates are shown for the fast kinetics of Scala, and for each of two thermochemical equilibria. Each experimental point is bracketed to indicate the estimated experimental error. Also, the theoretical curves are bracketed to indicate the uncertainty arising from estimated errors in the determination of the jet properties. The estimated errors are discussed in Appendix B.

F. COMPARISON WITH THE DATA OF DIACONIS, GORUSCH, AND SHERIDAN

Figure 10 shows the nondimensional results of the present experiments and those of Diaconis, Gorusch, and Sheridan (Ref. 9) that were recently published. The nondimensional combustion rate is defined as the ratio of

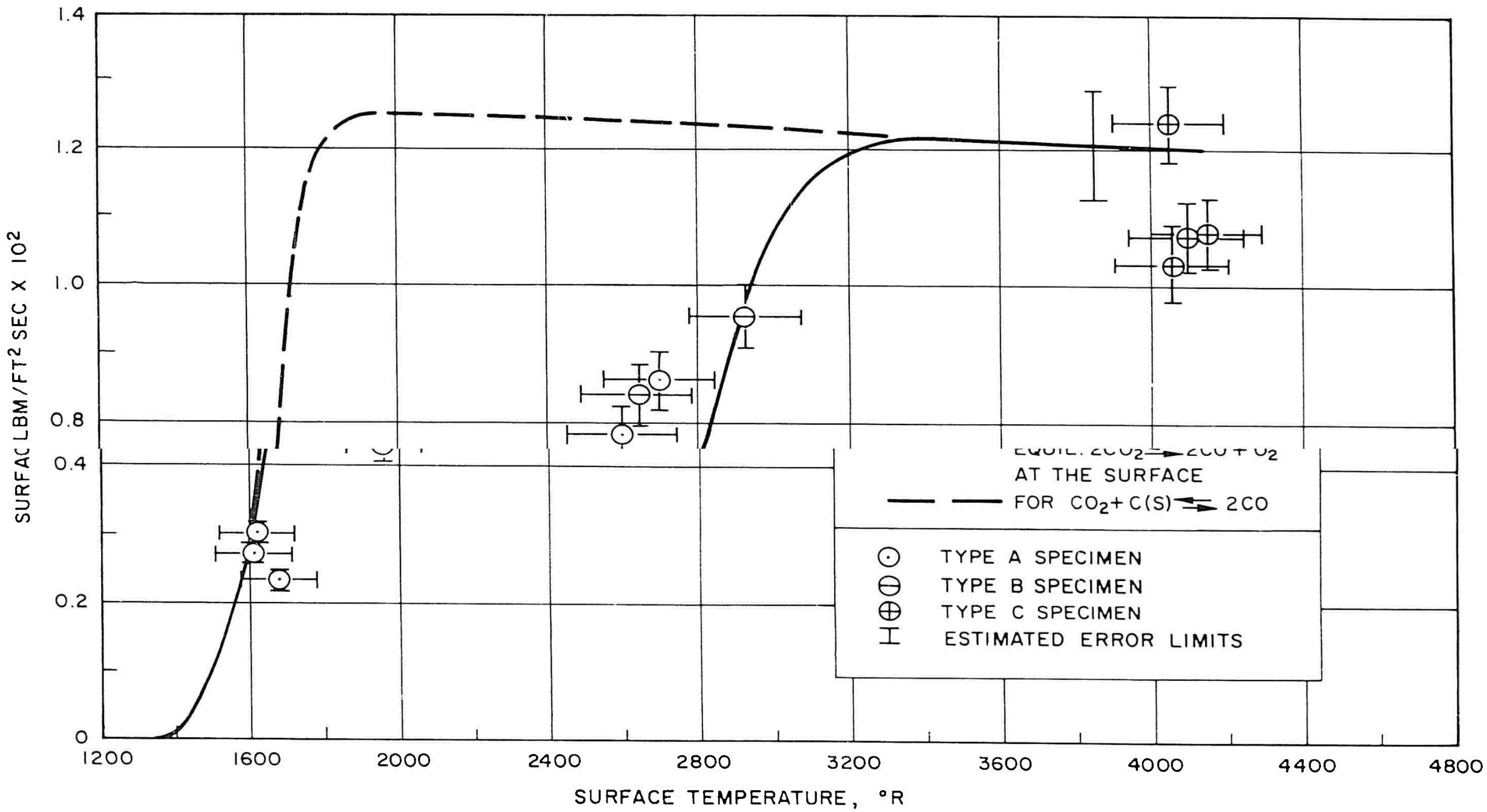

Fig. 9. Experimental Combustion Rates

the observed rate to the maximum (theoretical) diffusion-limited rate for CO production at the particular surface temperature. Theoretical results of Refs. 2 and 3 are shown for comparison. It is noted that the relation for Scala's fast kinetics, a one-half-order reaction, and the carbon-dioxide dissociative equilibrium appear to correspond closely to the data shown. A virtually contamination-free plasma arc was used by Diaconis, et al.; thus, it is apparent that the effect of cathode contamination in the present experiments was small.

G. COMPARISON WITH THE DATA OF GOLOVINA

The experimental combustion results of Golovina and Khaustovich (Ref. 10) offer an interesting comparison with the present results. Their data for oxygen reacting with graphite are shown as a shaded area in Fig. 10. The experimental apparatus consisted of a graphite sphere, heated by electric induction, over which either oxygen (in air) or carbon dioxide gases flowed. The gas flow was contained in a glass tube and was subsonic. The gas temperature was initially at room temperature. Since the average mass loss rate from a sphere is somewhat different than at the stagnation region, the data of Golovina are not directly comparable with the present results, but may be compared qualitatively on a nondimensional basis. The reference mass loss rate has been taken as the diffusion-limit for CO production, as shown in Ref. 10. Theoretical values of temperature for the intermediate regime- and product-transitions are essentially the same as those shown for the conditions of Diaconis.

It may be seen that the data of Golovina correspond closely to the results of the Type A, B, and C specimen tests, and to the data of Diaconis, from 2200 to 3200°R, but differ somewhat at the lower temperatures. This difference is in the intermediate regime, where Golovina's data lie about 400°R higher in temperature than the present results.

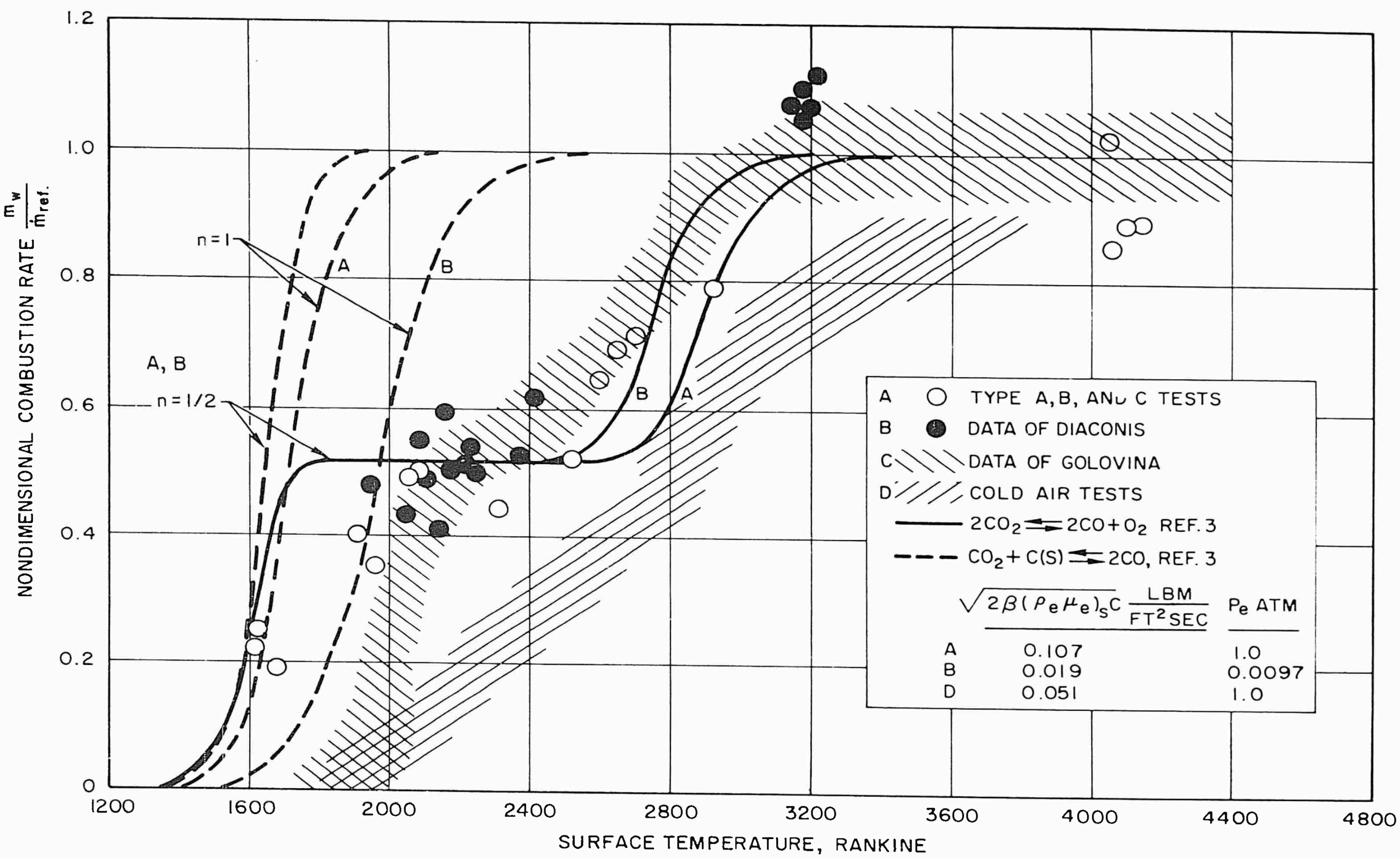

Fig. 10. Comparison with Other Investigations

Golovina and Khaustovich commented on the inflection of the combustion rate at intermediate temperatures, and suggested that this may be associated with a transition from CO_2 to CO production at the surface. They obtained a severe inflection in the reaction-rate using CO_2 as the gaseous reactant, which is unexplained at the present time.

H. COMPARISON WITH COLD-AIR DATA

In an attempt to establish whether the cathode-particle contamination and oxygen depletion existing in the tests using Type A, B, and C specimens might have caused some error in the combustion measurements, a brief series of tests using a cold-air jet was performed. These tests used what was essentially the reverse of the Type C specimen flow configuration, in that a hot plasma-arc flow of argon was used to heat one side of an ATJ-graphite disk, and a cold jet of air was used to burn the other side of the disk. The burning face of the disk was viewed directly with an optical pyrometer. These results are shown for comparison in Fig. 10, as a shaded area. Theoretical values of the intermediate regime- and product-transitions are essentially the same as shown for the main test series.

These cold-air test data appear to be displaced about $600^{\circ}R$ to a higher temperature than the results of the main test series, with the combustion rate undergoing a prolonged rise from zero to the CO diffusion limit over a temperature range of approximately $2000^{\circ}R$. It is not clear that the discrepancies between the cold- and hot-air data are the result of errors arising from the cathode particles in the hot-air tests. It is conceivable that fundamental differences exist in the kinetic phenomena at a burning carbon surface between the cases of a hot jet impinging on a cooler surface or a cold jet impinging on a hotter surface. That this might be the case may be seen by considering the diffusion and kinetic phenomena as they vary with local pressure and temperature in the pores beneath a carbon surface. Since the pores constitute a major fraction of the burning surface area, a reversed temperature gradient near the surface could effectively change the over-all kinetic behavior.

V. CONCLUDING REMARKS

The experimental data presented in this report indicate that (a) the theoretical solution of Refs. 2 and 3 for the diffusion-limited combustion rate is approximately valid, provided the effective product of combustion is known; (b) the fast kinetic relation of Scala (Ref. 1) correctly locates the temperature below which combustion of ATJ graphite becomes negligible compared to the diffusion-limited combustion rate; and (c) the surface thermochemical equilibrium $2CO_2 \leftrightarrows 2CO + O_2$ appears to be applicable, rather than $CO_2 + C(S) \leftrightarrows 2CO$, in the temperature range investigated.

The experimental errors stemming from the cathode-particle contamination present in this investigation appear not to be significant, in view of the favorable comparison with the recent results of Diaconis. Both investigations involve other sources of error, however, and the data scatter indicated in Fig. 10 serves to emphasize the need for additional experimental data in this temperature range. The data of Golovina and Khaustovich and the results of the brief series of tests using a cold-air jet indicate an extended temperature range over which the combustion rate varies, as in the tests using hot air, but at somewhat higher temperatures. This difference may result from a dependence of the surface kinetics on the direction of heat transfer at the surface, or from experimental errors of an undetermined nature.

Reaction-kinetic experiments by other investigators (discussed in Ref. 3) have failed to indicate a unique form for an empirical kinetic relation, even for a particular grade of graphite. This presents a problem in adequately describing the interaction between diffusion and kinetic effects, as was attempted in Ref. 3. The interaction was therefore described by arbitrarily utilizing the representative kinetic relations of Scala (Ref. 1), to permit a comparison with experimental results, even though the kinetics may be different for the particular material used in the experiments. Thus, the theoretical curves shown in this report do not necessarily indicate the correct temperatures at which one should expect the major variations in combustion rate for ATJ-graphite. At the present time, therefore, the comparisons shown here should be considered as qualitative and preliminary.

APPENDIX A

Theoretical Heat Flux and Combustion Rate Calculations

I. HEAT FLUX

Theoretical values of the stagnation-point heat flux for each test were calculated using the Fay and Riddle correlation:

$$q = \frac{0.763}{Pr^{0.6}} \left(\frac{\mu_w \rho_w}{\mu_s \rho_s}\right)^{0.1} (\beta \mu_s \rho_s)^{0.5} \left[1 + (Le^{0.63} - 1) \frac{h_D}{h_s}\right] (h_s - h_w) \tag{A-1}$$

The use of this correlation for the calculation of theoretical heat flux from a subsonic plasma jet to a stagnation-point surface upon which it impinges has been discussed by John and Bade (Ref. 5). They utilized the equation of state and the isentropic relation for real air to calculate the mean density and velocity of the jet, based on the stagnation pressure in the plasma-arc plenum and net power input to the gas. Also, the inviscid velocity gradient β near the stagnation point was taken by John and Bade as the ratio of the mean jet velocity to the exit nozzle diameter; this equivalence was indicated by pressure measurements at the stagnation surface. It can be shown that it is unnecessary to use the compressible relations for real air to evaluate Eq. (A-1). Since the inviscid velocity gradient is simply the mean jet velocity divided by the jet outlet diameter, Eq. (A-1) becomes

$$q = \frac{0.763}{Pr^{0.6}} \left(\frac{\bar{\rho}_s \bar{u}_s}{d_j}\right)^{0.5} (\mu_s)^{0.5} \left(\frac{\mu_w \rho_w}{\mu_s \rho_s}\right)^{0.1} \left[1 + (Le^{0.63} - 1) \frac{h_D}{h_s}\right] (h_s - h_w) \tag{A-2}$$

The measured rate of air mass flow input to the plasma arc may be utilized to evaluate the product of the mean density and velocity by simply dividing that rate by the exit-nozzle flow area. If the ratio of plenum-to-ambient pressures is kept near unity, the Mach number of the jet is low, and the stream viscosity, density, and enthalpy may be taken at the values for the stagnation condition at one atmosphere, with negligible error. The stagnation enthalpy was evaluated from the net electrical power input per unit mass of air flow per second. The property values for dissociated air were taken from Ref. 7; the Lewis number was taken as 1.4.

II. COMBUSTION RATE

Equation (17) of Ref. 3 shows that the diffusion-limited mass loss rate is

$$\dot{m}_{w,\,d.\,l.} = \frac{A_1 C_{1,\,e} \sqrt{(1+\epsilon)\beta(\rho_e\mu_e)_s C}}{Sc\,\dfrac{n_1 M_1}{n_w M_w} + A_2 C_{1,\,e}} \tag{A-3}$$

and Eq. (16) of that reference indicates that the mass loss rate in the kinetic regime is a function of these and additional kinetic variables. For the details of the calculation method the reader is referred to Ref. 3. The parameter $\sqrt{2\beta(\rho_e\mu_e)_s C}$ in Eq. (A-3) was calculated in a manner similar to that used in Eqs. (A-1) and (A-2), namely, by equating the inviscid velocity gradient to the ratio of mean jet velocity to jet diameter and substituting the mass flow per unit area for the velocity-density product.

APPENDIX B

Estimation of Experimental Errors

I. SPECIMEN COMBUSTION RATE

The combustion rate was calculated by the relation

$$\dot{m}_w = \rho_g(\Delta L/\Delta t)$$

The errors estimated to exist are

Symbol	Description	Measured By	Estimated Error, %
ρg	Graphite density	Chemical balance	±1
ΔL	Specimen length loss	Vernier calipers	±2
Δt	Test time	Stop watch	±2
			±5 Total

II. SPECIMEN SURFACE TEMPERATURE

A. Type A Specimen

T_s computed by measurements of temperature near the rear face, heat load through the specimen, and calculation of conduction through graphite, in finite numerical increments to allow for variation of k with T. The thermal conductivity data of Armour Research for commercial graphite were taken as listed in Ref. 11. The surface temperature was obtained with the relation

$$T_s = T(x_a) + \sum_{i=1}^{n} q\frac{(L - x_a)}{nk(\bar{T}_i)}$$

The errors estimated to exist are

Symbol	Description	Measured By	Estimated Error
$T(x_a)$	Temperature near cooled face	Thermocouple, recording potentiometer	$\pm 10^{\circ}F$
q	Heat flux through specimen	Water-cooled calorimeter	±5%
$L - x_a$	Modified specimen length	Vernier calipers	±2%
n	No. of increments (usually eight or more)	----	---
k	Thermal conductivity	(see Ref. 9)	±5%
			±12% ± $10^{\circ}F$

The temperature difference $T_s - T(x_a)$ was on the order of 1000°F. Thus, the order of error in surface temperature calculated is 130°F for Type A specimens.

B. Type B Specimen

Surface temperature was calculated in a manner similar to that used for Type A specimens, except that additional computation increments were provided because of increased specimen length. The rear face temperature was estimated to be 30°F above the saturation temperature of the calorimeter cooling water, and this was verified within 30°F in a preliminary test with an internal thermocouple in a specimen. Approximately 15 percent of the incoming heat flux to the front surface was estimated to be diverted to the guard plate, so the calculation procedure had to be modified for non-one-dimensional heat flow based on a measurement of internal specimen temperature near the heated surface. Also, a small correction was made for radiative loss from the circumference of each computation segment. These modifications were necessarily crude, and the over-all error is estimated to be about $\pm 150^{o}F$, somewhat greater than with the Type A specimen.

C. Type C Specimen

The surface temperatures of Type C specimens were measured with a manual monochromatic pyrometer at 0.65 microns wavelength. The emissivity correction was insignificant because of the high emissivity of graphite. The combined errors of imperfect luminosity matching by the operator and inherent instrument errors are estimated to be within $\pm 150^{o}R$ at $4100^{o}R$.

III. ARC OPERATING CONDITIONS

Variations and uncertainties in the arc operating conditions for these experiments affected the consistency of comparison of experimental combustion rates at various surface temperatures and the accuracy of the calculations of theoretical values of heat transfer and mass loss rates. The significant parameter determined by the arc conditions for mass loss rate is

$$\sqrt{2\beta(\rho_e\mu_e)_s C} \qquad \text{or} \qquad \sqrt{\frac{8\dot{m}_j}{\pi d_j^3}\mu_e C}$$

The estimated errors are

Symbol	Description	Measured by	Estimated Error, %
$\dot{m}_j$	Air flow rate	Bourdon-recorder	±3
d_j	Exit diameter	Vernier calipers	±1.5
μ_e	Mean jet viscosity	(enthalpy measurement and Ref. 7)	±1
C	Density-viscosity ratio	(surface temperature, enthalpy)	±0.5
		Total	±6

In addition to these indeterminate errors, small variations in air flow rate and enthalpy occurred, amounting to a ±3.7 percent determinate variation in the square-root parameter. Thus, taking one-half of the indeterminate error in terms appearing inside the square root term and adding the determinate variation, the expected range of applicability of an average value of this term is +6.7 percent.

The square-root parameter above is also a major term in the calculation of theoretical heat flux. Heat flux (see Eq. A-2) also includes the enthalpy difference $(h_s - h_w)$. The stagnation enthalpy was determined by the relation

$$h_s = \frac{\text{Gross Power into Arc minus Cooling Losses}}{\text{Air Mass Flow Rate}}$$

A facility calibration recently performed has indicated that stagnation enthalpy may be determined with an average accuracy of about ±7 percent by this method. Thus, the theoretical heat flux for a particular test was accurate to within ±10 percent, adding the indeterminate error in the square-root term to the enthalpy uncertainty. As noted in subsection IV-B, the comparison of experimental and theoretical heat flux indicates that the arc instrumentation suffered spurious changes in some tests, yielding erroneously low indicated enthalpy values, by about 20 percent.

REFERENCES

1. Scala, S. M., "The Ablation of Graphite in Dissociated Air. Part I: Theory," IAS Paper No. 62-154 (19 June 1962).

2. Welsh, W. E., Jr., and Chung, P. M., "An Analysis of the Effects of Heterogeneous Reaction Kinetics on the Combustion of Graphite at the Stagnation Region of a Blunt Body in Hypersonic Flow," TDR-169(3230-12)TN-6, Aerospace Corporation, El Segundo, Calif. (28 February 1962).

3. Welsh, W. E., Jr. and Chung, P. M., "A Modified Theory for the Effect of Surface Temperature on the Combustion Rate of Carbon Surfaces in Air," Proceedings of the 1963 Heat Transfer and Fluid Mechanics Institute, 12-14 June 1963.

4. Grabowsky, W. R., and Spencer, D. J., "High Temperature Arc Studies," TR 69-0000-09934, Space Technology Laboratories, Redondo Beach, Calif. (31 December 1959).

5. John, R. R., and Bade, W. L., "Stagnation Point Heat Transfer in a Subsonic Jet of Arc-Heated Air," ARS Journal (July 1959), 523-24.

6. Horn, R. C., and Lafazan, S., "High Mach Number and Materials Research Program, Phase II, Arc Plasma Investigations and Arc Tunnel Materials Studies," Semiannual Technical Report 1 January-30 June 1961, TDR-594(1206-01)STR, Vol. II, Aerospace Corporation, El Segundo, Calif.

7. Hansen, C. F., "Approximations for the Thermodynamic and Transport Properties of High Temperature Air," NASA TR-R-50 (1959).

8. Carslaw, H. S., and Jaeger, J. C., Conduction of Heat in Solids. (Oxford, Clarendon Press, 1947), p. 104.

9. Diaconis, N. S., Gorsuch, P. D., and Sheridan, R. A., "The Ablation of Graphite in Dissociated Air. Part II: Experiment," IAS Paper No. 62-155 (19 June 1962).

10. Golovina, E. S., and Khaustovich, G. P., "The Interaction of Carbon with Carbon Dioxide and Oxygen at Temperatures up to 3000°K," Proceedings of the Eighth Symposium on Combustion, 28 August-3 September 1960 (Williams and Wilkins, New York, 1962).

11. Nolan, E. J., and Scala, S. M., "The Aerodynamic Behaviour of Pyrolytic Graphite During Sustained Hypersonic Flight," R61SD051, General Electric Co. (March 1961).

AEROSPACE CORPORATION

TECHNICAL REPORTS - DISTRIBUTION LIST

REPORT TITLE
"Experimental Results on the Combustion Rate of Graphite Exposed to a Plasma-Arc Flow"

REPORT NO.	DATE	SECURITY CATEGORY
TDR-269(4230-40)-1	31 August 1963	Unclassified

EXTERNAL DISTRIBUTION

MILITARY AND GOVERNMENT OFFICES

NASA

National Aeronautics and Space Admin.
Langley Research Center
Langley Field, Va.

National Aeronautics and Space Admin.
Lewis Research Center
Attn: Library
21000 Brookpark Road
Cleveland 35, Ohio

NASA
Ames Research Center
Moffett Field, California
Attn: Library

NAVY

Commander
U. S. Naval Ordnance Laboratory
Attn: Library
White Oak
Silver Spring, Maryland

Commanding Officer and Director
David Taylor Model Basin
Aerodynamics Laboratory
Attn: Library
Washington 7, D. C.

Rand Corporation
1700 Main Street
Santa Monica, Calif.

ASSOCIATE CONTRACTORS AND OTHER

EDUCATIONAL INSTITUTIONS

Brown University
Division of Engineering
Attn: Library
Providence 12, Rhode Island

Brooklyn Polytechnic Inst.
Schermerhorn St.
Brooklyn, N. Y.

Princeton University
Department of Aero. Engineering
Attn: Library
Princeton, N. J.

Rensselaer Polytechnic Institute
Dept. of Aeronautical Eng.
Attn: Library
Troy, New York

The University of Southern Calif.
Engineering Center
Attn: Librarian
University Park
L. A. 7, Calif.

Stanford University
Dept. of Aeronautical Eng.
Attn: Library
Stanford, California

University of Michigan
Dept. of Aeronautical Engineering
Attn: Prof. A. Kuethe
Ann Arbor, Michigan

Ohio State University
Aeronautical Engineering Dept.
Columbus, Ohio

INSTRUCTIONS

WHEN APPROVED BY GOVERNMENT PROGRAM OFFICE, LINE OUT UNUSED SPACE TO PRECLUDE ADDITIONAL ENTRIES.

PREPARED BY W. E. Welsh Jr. (FOR AEROSPACE CORPORATION) J. Logan

APPROVED BY G. S. Lewis, Jr. Maj. USAF (FOR GOVERNMENT PROGRAM OFFICE)

(USE ADDITIONAL PAGES AS NECESSARY)

AEROSPACE FORM 2380

AEROSPACE CORPORATION

TECHNICAL REPORTS – DISTRIBUTION LIST

REPORT TITLE		
"Experimental Results on the Combustion Rate of Graphite Exposed to a Plasma-Arc Flow"		
REPORT NO. TDR-269(4230-40)-1	DATE 31 August 1963	SECURITY CATEGORY Unclassified

EXTERNAL DISTRIBUTION

MILITARY AND GOVERNMENT OFFICES	ASSOCIATE CONTRACTORS AND OTHER
SSD (SSTRE) Spacecraft Configuration & Performance Branch AF Unit Post Office Los Angeles 45, Calif	Purdue University School of Aeronautical Engineering Attn: Library Lafayette, Indiana
SSD (SSTP/Capt Debus) AF Unit Post Office Los Angeles 45, Calif	Aeronautics Library The John Hopkins University Baltimore 18, Maryland
AFCRL (ERD Library) LG Hanscom Fld Bedford, Mass	Massachusetts Institute of Technology Dept. of Aeronautics and Astronautics Library, Building 33 Cambridge 39, Massachusetts
AFCRL (CRRB) LG Hanscom Fld Bedford, Mass	University of Maryland Attn: Engineering Library College Park, Maryland
AF Ofc of Scientific Rsch (Library) Wash 25 DC	University of Minnesota Institute of Technology Attn: Engineering Library Minneapolis, Minnesota
Hq, DDC Bldg 5 Cameron Stn Alexandria, Va	Aeronautics Library Guggenheim Aeronautical Laboratory California Institute of Technology Pasadena 4, California
OSD (DDR&E) Info Ofc, Library Br Wash 25 DC	Engineering Library University of California 405 Hilgard Avenue Los Angeles 24, California
AFWL (Library) Kirtland AFB Albuquerque, New Mexico	Mechanical Engineering Library Case Institute of Technology University Circle Cleveland 6, Ohio
Library of Congress Wash 25 DC	Cornell Aeronautical Laboratory, Inc. P. O. Box 235 Buffalo 21, N. Y.
Hq NASA 400 Maryland Avenue, S.W. Wash 25 DC	
NASA (Library) Marshall Space Flight Center Huntsville, Alabama	

INSTRUCTIONS	
WHEN APPROVED BY GOVERNMENT PROGRAM OFFICE, LINE OUT UNUSED SPACE TO PRECLUDE ADDITIONAL ENTRIES.	PREPARED BY W. E. Welsh Jr. (FOR AEROSPACE CORPORATION) APPROVED BY G S Lewis Jr. Maj. USAF (FOR GOVERNMENT PROGRAM OFFICE)

(USE ADDITIONAL PAGES AS NECESSARY)

AEROSPACE FORM 2380

AEROSPACE CORPORATION

TECHNICAL REPORTS – DISTRIBUTION LIST

REPORT TITLE
"Experimental Results on the Combustion Rate of Graphite Exposed to a Plasma-Arc Flow"

REPORT NO.	DATE	SECURITY CATEGORY
TDR-269(4230-40)-1	31 August 1963	Unclassified

EXTERNAL DISTRIBUTION

MILITARY AND GOVERNMENT OFFICES

National Bureau of Standards (Library)
Wash 25 DC

Naval Research Lab
Director, Tech Info Ofcr
Code 2000
Wash 25 DC

Oak Ridge National Lab (Library)
P. O. Box Y
Oak Ridge, Tennessee

Office of Technical Services
Technical Reports Section
Department of Commerce
Wash 25 DC

ONR Branch
Commanding Officer
1030 Green Street East
Pasadena, California

RADC (Library)
Griffis AFB, New York

US Army Signal R&D Lab (Data Equip Br)
Technical Information Officer
Fort Monmouth, New Jersey

US Atomic Energy Commission (Director of Rsch)
Wash 25 DC

US Atomic Energy Commission
Tech Info Service Extension
P. O. Box 62
Oak Ridge, Tennessee

US Naval Rsch Lab (Library)
Wash DC

ASSOCIATE CONTRACTORS AND OTHER

Grad. School of Aerospace Eng.
Grumman Hall, Cornell University
Ithaca, N. Y.

INDUSTRIAL ORGANIZATIONS

AVCO Manufacturing Company
Research and Advanced Development Division
Attn: Research Library, Mrs. H. M. Page
201 Lowell St.
Wilmington, Massachusetts

AVCO-Everett Research Lab.
2385 Revere Beach Parkway
Everett 49, Mass.

Boeing Airplane Co.
Attn: Library
P. O. Box 3107
Seattle 14, Washington

Jet Propulsion Laboratory
4800 Oak Grove Drive
Pasadena, California
Attn: Library

Douglas Aircraft Co.
Missiles and Space Systems Eng. Lab.
Santa Monica Division
Santa Monica, Calif.

General Electric
Aeroscience Lab. - MSVD
Attn: Library (Please route to Dr. H. Lew)
3750 "D" Street
Philadelphia 24, Pennsylvania

RIAS Inc.
Attn: Library
7212 Bellona Ave.
Baltimore 12, Maryland

INSTRUCTIONS

WHEN APPROVED BY GOVERNMENT PROGRAM OFFICE, LINE OUT UNUSED SPACE TO PRECLUDE ADDITIONAL ENTRIES.

PREPARED BY W. E. Welsh Jr (FOR AEROSPACE CORPORATION)

APPROVED BY G. S. Lewis Jr. Maj. USAF (FOR GOVERNMENT PROGRAM OFFICE)

(USE ADDITIONAL PAGES AS NECESSARY)

AEROSPACE FORM 2380

AEROSPACE CORPORATION

TECHNICAL REPORTS – DISTRIBUTION LIST

REPORT TITLE
"Experimental Results on the Combustion Rate of Graphite Exposed to a Plasma-Arc Flow"

REPORT NO.	DATE	SECURITY CATEGORY
TDR-269(4230-40)-1	31 August 1963	Unclassified

EXTERNAL DISTRIBUTION

MILITARY AND GOVERNMENT OFFICES

Wright Air Development Center (Library)
Wright-Patterson AFB, Ohio

Flight Dynamics Laboratory
Research & Technology Division
Wright-Patterson AFB, Ohio

Hq, BSD
Ballistic Missile Re-Entry Systems Office
Norton AFB, San Bernadino, Calif

Hq, Research & Technology Division
Scientific & Technical Liaison Office
Bolling AFB, Wash 25 DC

National Bureau of Standard (2)
Boulder Laboratories
Boulder, Colorado

SSTP - Capt D. De Bus

Defense Documentation Center (20)
Cameron Station
Attn: TISIA
Alexandria, Virginia - 22314

Scientific and Technical Information (2)
Facility
Attn: NASA Repeesentative (SAK/DL-841)
PO Box 5700
Bethesda, Maryland, 20014

ASSOCIATE CONTRACTORS AND OTHER

The Martin Company
Aerophysics Research
Mail J 3-33
Baltimore 3, Md.

Lockheed Aircraft Missile Systems
Division
Attn: Library
Palo Alto, Calif.

Space Technology Laboratories
1 Space Park
Redondo Beach, Calif.
Attn: Librarian

JOURNALS

ARS Journal
Technical Literature Digest
500 Fifth Avenue
New York 36, New York

Institute of Aeronautical Sciences
Attn: Library
2 East 64th Street
New York 21, New York

Southwest Research Institute
Attn: Applied Mechanics Reviews
8500 Culebra Road
San Antonio 6, Texas

INSTRUCTIONS

WHEN APPROVED BY GOVERNMENT PROGRAM OFFICE, LINE OUT UNUSED SPACE TO PRECLUDE ADDITIONAL ENTRIES.

PREPARED BY W. E. Welsh (FOR AEROSPACE CORPORATION)

APPROVED BY G. S. Lewis, Jr. Maj. USAF. (FOR GOVERNMENT PROGRAM OFFICE)

(USE ADDITIONAL PAGES AS NECESSARY)

AEROSPACE FORM 2380

AEROSPACE CORPORATION

TECHNICAL REPORTS - DISTRIBUTION LIST

REPORT TITLE		
"Experimental Results on the Combustion Rate of Graphite Exposed to a Plasma-Arc Flow"		
REPORT NO. TDR-269(4230-40)-1	DATE 31 August 1963	SECURITY CATEGORY Unclassified

INTERNAL DISTRIBUTION

J. G. Logan

M. L. Rosenzweig

D. J. Spencer

W. R. Grabowsky

S. Lafazan

G. R. Inger

O. Kramer

R. A. Hartunian

J. Quinville

R. L. Varwig

N. Rott

J. Solomon

H. Mirels

Note: Please deliver 20 copies to the author.

Library/SBO (2)

Library/ESO (2)

Library/PAFB
(Badillo)

Publications/ESO
(Saltzman)

Reports Control/ESO (10 and vellum)

PREPARED BY W. E. Welch Jr.

AEROSPACE FORM 2394